sciendo

DOI 10.2478/ama-2024-0023

acta mechanica et automatica, vol.18 no.2 (2024)

# MATHEMATICAL ANALYSIS OF CHEMICALLY REACTING SPECIES AND RADIATION EFFECTS ON MHD FREE CONVECTIVE FLOW THROUGH A ROTATING POROUS MEDIUM

**Pawan Kumar SHARMA*, Bhupendra Kumar SHARMA**, Anil KUMAR***

*Amity Institute of Applied Sciences, Amity University, Amity Road, Sector 125, Noida, Utter Pradesh – 201303, India
**Department of Mathematics, Birla Institute of Technology and Science, Pilani, Rajasthan – 333031, India

pksharma@amity.edu, bhupen_1402@yahoo.co.in, akumar35@amity.edu

*received 2 May 2023, revised 3 August 2023, accepted 28 August 2023*

**Abstract:** The present study deals with the effects of radiation and mass transfer on a laminar unsteady free convective flow of a viscous, incompressible, electrically conducting and chemically reacting fluid past a vertical surface in a rotating porous medium. It is assumed that the surface is rotating with angular velocity $\Omega$. The governing mathematical equations are developed and solved by adopting complex variable notations and the analytical expressions for velocity, temperature and concentration fields are obtained. The effects of various parameters on mean primary velocity, mean secondary velocity, mean temperature, mean concentration, transient primary velocity, transient secondary velocity, transient temperature and transient concentration have been discussed and shown graphically. Further, the consequences of different parameters on rate of heat transfer coefficient (Nusselt number), rate of mass transfer coefficient (Sherwood number) and drag coefficient (mean skin-friction) are analysed. It is observed that the mean and transient primary velocities increase with the radiation parameter E, while reverse phenomena are observed for the Schmidt number, Sc, and the chemical reaction parameter, $\gamma$. The results may be useful in studying oil or gas and water movement through an oil or gas field reservoir, underground water migration, and the filtration and water purification processes.

**Key words:** porous medium; MHD; chemically reacting fluid, radiation, heat transfer, mass transfer

## 1. INTRODUCTION

In several trades of science and engineering, the impact of the chemical reaction along with the transfer of heat and mass is studied, since it has a significant practical importance among scientists and engineers. First of all, the combinatorial buoyancy effects were investigated, and we found that it imparts the naturalistic convective flows adjoining together with the upright and flat surfaces of the thermal and mass diffusion. In the realm of theoretical investigation, the dynamic interplay of magnetohydrodynamics and rotational forces unveils its enigmatic balance with a viscous, incompressible fluid cascading over a vertical plate ensconced within a porous medium [1–5]. The impact of the varying concentration and temperature of the surface extensively on the naturalistic convective flow for an upright flat surface was studied extensively. The flow model functions as a cooling agent at the surface, leading to a reduction in the concentration of the diffusing species at the boundary. The presence of an applied magnetic field, thermal radiation, porosity in the saturated porous medium, and a chemically reactive process all contribute to the gradual thinning of the boundary layer [6, 7]. The analysis of the thermal along with mass diffusion simultaneously was reported for the mixed type of convection flows via a perforated median. Increasing both the heat source parameter and the radiation quantity leads to a heightened concentration of temperature distribution. On the other hand, elevating one of the chemical reaction parameters causes a reduction in concentration throughout the entire fluid region. Manipulating the rotation parameter can decrease skin-friction, but it may worsen the Hall effect and ion slip effect. Interestingly, augmenting the chemical reaction parameter results in a simultaneous increase in the mass transfer rate [8–11]. The impacts of varying temperature and concentration were found over the free convective stream flow in unsteady state condition passed on an upright surface with infinite length and static state of suction. The role of chemical reactions and activation energy holds immense significance in analysing the behaviour of fluid dynamics and its thermal characteristics [12–15]. The analysis delves into the application of fluid flow in various domains, including nuclear reactors, automobiles, manufacturing setups and electronic appliances. Specifically, when both the Darcy–Forchheimer and activation energy parameters are elevated, the velocity and concentration of the fluid decrease. This implies a delicate balance between these factors in the overall behaviour of the system under investigation. The impact of the heat along with mass transport on the blood flow model having two-phase has been represented and discussed in the analogous literature. Investigation is conducted into the dynamic behaviour of an unsteady flow of a viscous liquid subjected to an induced magnetic field while being controlled through uniform suction [16–19]. The nalysis addresses the thermal equation, radiation, and entropy rate in the thermodynamic system. These results provide valuable insights into the intricate interplay between the thermal and magnetic fields, entropy production, concentration and velocity. By approaching this complex problem in a unique way, the prevailing understanding into how different physical variables interact and influence the overall behaviour of the system under investigation was studied.

In the progressions containing higher temperatures, the transfer of heat through radiation along with the impact of convective

heat transfer as well as mass transfer has a significant role in the designing and development of key equipment used in the fields, for instance gas turbines power generation plants, nuclear power plants and the numerous propulsive tactics used in the area of aerospace such as aircraft, satellites, space shuttles and missiles. The impacts of radiation were represented for the free convective stream flow over the hemi-infinite past porous surface along with the transfer of the mass. The numerical values of physical quantities, such as the local skin-friction coefficient, the local Nusselt number and the local Sherwood number, were also calculated in a clear and organised way [20–25]. The transfer of heat was evaluated under a thermally radiative medium, while the transfer of mass for an upright surface in the moving condition. The impacts of heat and mass transfer were explored on the free convective flow of a micropolar fluid adjacent to an infinite vertical porous plate [26–29]. The significance of this research extends to diverse fields such as geophysics, medicine, biology and any processes that benefit from a strong magnetic field in a low-density gas environment. The impact of the radiation along with the transfer of mass was also investigated over an isothermal upright surface under the two-dimensional flow. The introduction of coordinate and parametric transformations in the governing equations has revealed remarkable insights that have seldom been reported in the literature [30–32]. The investigation has yielded crucial findings, particularly concerning the impact of the Ergun number on various fluid types. Interestingly, the Ergun number has demonstrated its ability to reduce the velocity boundary layer of pseudoplastic fluids, a highly desirable outcome. However, it has been observed to enhance the thermal boundary layer in these fluids. In contrast, for Newtonian and dilatant fluids, this effect has proven to be relatively insignificant. The unsteady convectional flow by means of the rotating perforated median with the radiational effect and periodic flux of heat was reported significantly [33, 34].

MHD is an important aspect in covering the mechanical properties of the liquid in the fluid dynamics and deals with the cooperation among the electrically conductive and electromagnetic fluids. The flows involved in the fluids that are a good conductor of the electricity subjected to the effect of the magnetic field have drawn the attention of various investigators due to their uses in astrophysics, geophysics, engineering applications and the control of aerodynamic boundary layer. The MHD free convective stream flows were assessed for a plate put at heat flux with oscillations of surface. The unsteady free convection flow of a viscous incompressible fluid delved through a highly porous medium, bounded by a vertical infinite moving plate, has been discussed by many researchers [35–39]. During the evaluation of the intricate interplay of thermal diffusion, chemical reaction and heat source, it is necessary to consider all of these as being under the influence of the Soret effect. The fluid is grey, absorbing and emitting, and yet non-scattering, adding complexity to the problem. This research sheds light on the complex dynamics of fluid flow through porous media, offering valuable implications for various practical applications and opening doors to further investigations in this captivating area of study. The transport of heat along with mass was clarified in the magneto-biofluid flow with Joule effect via a non-Darcian porous medium [40, 41].

Extensive investigations of the magnetohydrodynamic mixed convective stream flow passing through the upright flat surface were organised under the numerous applications of MHD flow through the porous type of medium. In a comprehensive investigation [42–46], the combined influences of Soret and Joule effects were thoroughly analysed on the magnetohydrodynamic mixed convective flow of an electrically conducting, incompressible and viscous fluid past an infinite vertical porous plate. The unique exploration provided valuable insights into the complex dynamics of MHD mixed convective flows, particularly in the presence of porous media and Hall effects. These findings are significant for various engineering applications, especially those involving heat and mass transfer phenomena. The state of the unsteady flow for free convective stream was represented under the thermal as well as mass diffusion in the environment of Hall impact. The influence of Hall current on the unsteady free convection flow of an electrically conducting, viscous incompressible fluid was explored [47–49]. The flow occurred past a fluctuating porous flat plate, with internal heat absorption/generation, and in the presence of foreign gases. The study considered various parameters, including the Hall current, the hydromagnetic parameter, the Grashoff number for heat transfer, the Grashoff number for mass transfer, the internal heat absorption/generation parameter, the transpiration parameter, the Schmidt parameter and the chemical reaction parameter. Overall, this investigation contributes valuable insights into the intricate interactions between Hall current, magnetic force, thermal buoyancy and heat generation/absorption, enriching our understanding of complex fluid dynamics and heat transfer phenomena. The effect of MHD on unsteady oscillatory Couette flow through porous media and the influence of the radiation and related chemical reactions were also investigated in an unsteady state magnetohydrodynamic free convection flow with the transfer of mass over a heated upright porous surface rooted in highly porous type of median [50, 51]. The unsteady natural oscillatory convective Couette flow was demonstrated via a variable perforated type of median with the effect of chemical species concentration [52, 53]. Under the presumption of varying permeability, the impact of related chemical reactions on the flow of micropolar fluid reported the replication of the microscopic effects owing to the local behaviour and micro-motion of the liquid particles. The influence of Joule heating on the steady two-dimensional flow of an incompressible micropolar fluid over a flat deformable sheet was investigated [54–56], with the investigation uncovering that the presence of second-order slip plays a constructive role in ensuring flow stability, during both the stretching and shrinking of the deformable surface. Overall, these insightful results contribute to our understanding of the interplay between Joule heating and micropolar fluid flow over deformable sheets, offering potential implications in diverse fields, ranging from engineering applications to scientific advancements. Recently, the impact of species chemical reactivity as well as the prevalence of radiation over the MHD flow through a relocating perpendicular perforated flat surface, together with that of the source of heat and suction, has been evaluated in the analogous research literature. The behaviour of a two-dimensional incompressible magnetohydrodynamic fluid flowing over a linear stretching sheet was investigated considering the effects of suction or injection and convective boundary conditions [57, 58]. To analyse the system, a scaling group transformation method was employed, which helps simplify the governing equations by revealing certain invariance properties. These studies contribute to a deeper understanding of the intricate fluid dynamics in the presence of magnetic fields and various boundary conditions, and the achieved agreement validates the reliability of the utilised numerical approach.

This research paper introduces a novel study of the combined effects of radiation and chemical reactions in a rotating porous medium. It investigates the impact of a magnetic field on unsteady state natural convective chemically reacted flow over an infinite

upright plate, considering a revolving condition with a permeable median. The inclusion of periodic thermal and mass diffusion at the upright surface adds complexity. The study employs a regular perturbation method to obtain investigational solutions for flow characteristics. The findings are presented graphically, providing a clear visualisation of the influence of different parameters on flow-related characteristics. This comprehensive analysis offers valuable insights into fluid dynamics and heat transfer in this unexplored scenario.

## 2. MATHEMATICAL FORMULATION

We considered the unsteady viscous incompressible flow through electrically conducting and chemically reacting the fluid by means of a foraminate median, inhabiting a hemi-infinite area of space confined by an upright endless foraminate plate in a revolving tract, when the temperature and mass flux of the plate area change with respect to the length of time. Now we assume the impact of radiations on an upright plate that is under a similar static magnetic field and suction velocity, which are exerted in a directional way that is vertical to the surface. An upright endless foraminate plane area revolving around a perpendicular axis of a vertical plane with the constant angular velocity Ω subjected to a viscous fluid embedded in porous medium is considered. At the $z^* = 0$ plane, a vertical porous plane is considered with the $z^*$-axis perpendicular to this plane. The $x^*$-axis is considered in a perpendicular upward direction while the $y^*$-axis is in the normal direction to the $z^* = 0$ plane. The stream flow is considered to be along with the plane $z^* = 0$. The schematic of flow configuration is given in Fig. 1. Now, considering the above assumptions, all the physical variable quantities, excluding the pressure 'p', are only the function of direction $z^*$ and time $t^*$.

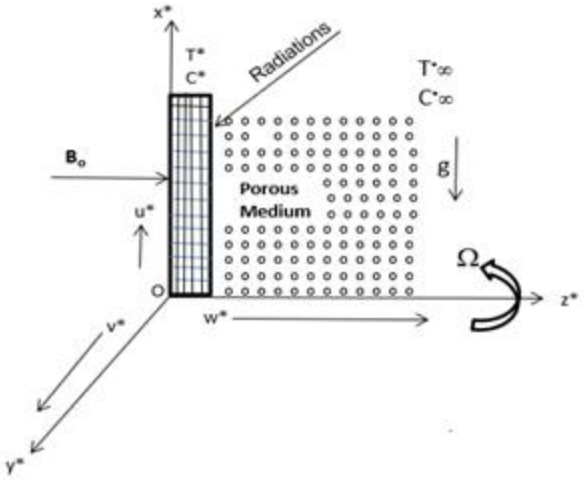


**Fig. 1.** Schematic of flow configuration

The mass and momentum conservation equations along with the transfer of energy in the revolving frame are specified below [50]:

$$\frac{\partial w^*}{\partial z^*} = 0, \tag{1}$$

$$\frac{\partial u^*}{\partial t^*} + w^* \frac{\partial u^*}{\partial z^*} - 2\Omega v^* = g\beta(T^* - T_\infty^*) + g\beta'(C^* - C_\infty^*) + \nu \frac{\partial^2 u^*}{\partial z^{*2}} - \frac{\nu\, u^*}{k^*} - \frac{(\vec{J}\times\vec{B})}{\rho}, \tag{2}$$

$$\frac{\partial v^*}{\partial t^*} + w^* \frac{\partial v^*}{\partial z^*} + 2\Omega u^* = \nu \frac{\partial^2 v^*}{\partial z^{*2}} - \frac{\nu v^*}{k^*} - \frac{(\vec{J}\times\vec{B})}{\rho}, \tag{3}$$

$$0 = -\frac{1}{\rho}\frac{\partial p^*}{\partial z^*} - \frac{\nu w^*}{k^*} - \frac{(\vec{J}\times\vec{B})}{\rho}, \tag{4}$$

where the terms of the right-hand side from Eq. (2) to Eq. (4) represent the occurrence of the Lorentz force attributable to the magnetic field '$\vec{B}$', which is specified by:

$$\vec{J}\times\vec{B} = \sigma(\vec{v}\times\vec{B})\times\vec{B} \tag{5}$$

Putting the value of Eq. (5) in Eqs (2)–(4), the resultant new forms of equations are given by:

$$\frac{\partial u^*}{\partial t^*} + w^* \frac{\partial u^*}{\partial z^*} - 2\Omega v^* = g\beta(T^* - T_\infty^*) + g\beta'(C^* - C_\infty^*) + \nu \frac{\partial^2 u^*}{\partial z^{*2}} - \frac{\nu\, u^*}{k^*} - \frac{\sigma B^2}{\rho} u^*, \tag{6}$$

$$\frac{\partial v^*}{\partial t^*} + w^* \frac{\partial v^*}{\partial z^*} + 2\Omega u^* = \nu \frac{\partial^2 v^*}{\partial z^{*2}} - \frac{\nu v^*}{k^*} - \frac{\sigma B^2}{\rho} v^*, \tag{7}$$

$$0 = -\frac{1}{\rho}\frac{\partial p^*}{\partial z^*} - \frac{\nu w^*}{k^*} - \frac{\sigma B^2}{\rho} w^*, \tag{8}$$

$$\frac{\partial T^*}{\partial t^*} + w^* \frac{\partial T^*}{\partial z^*} = \alpha \frac{\partial^2 T^8}{\partial z^{*2}} - \frac{1}{\rho C_p}\frac{\partial q_r^*}{\partial z^*}, \tag{9}$$

$$\frac{\partial C^*}{\partial t^*} + w^* \frac{\partial C^*}{\partial z^*} = D \frac{\partial^2 C^*}{\partial z^{*2}} - k_1(C^* - C_\infty^*). \tag{10}$$

The boundary conditions of the problem are as below:

$$\left.\begin{array}{l} z = 0 .u^* = 0,\ v^* = 0,\ \frac{\partial T^*}{\partial z^*} = -\frac{q_w^*}{\kappa}(1 + \varepsilon e^{i\omega^* t^*}), \\ \frac{\partial C^*}{\partial z^*} = -\frac{m_w^*}{D}(1 + \varepsilon e^{i\,\omega^* t^*}) \\ z \to \infty: u^* \to 0, v^* \to 0, T^* \to T_\infty^*, C^* \to C_\infty^*. \end{array}\right\} \tag{11}$$

For the constant value of the suction, from Eq. (1), we obtain:

$$w = -w_0 \tag{12}$$

Assuming u + iv = U with Eq. (12), Eqs (6) and (7) can be written as:

$$\frac{\partial U^*}{\partial t^*} - w_0 \frac{\partial U^*}{\partial z^*} + 2i\Omega U^* = g\beta(T^* - T_\infty^*) + g\beta'(C^* - C_\infty^*) + \nu \frac{\partial^2 U^*}{\partial z^{*2}} - \frac{\nu U^*}{k^*} - \frac{\sigma B^2 U^*}{\rho} \tag{13}$$

Now, we introduce the dimensionless quantities, as the following:

$$z = \frac{w_0 z^*}{\nu}, U = \frac{U^*}{w_0},\ t = \frac{t^* w_0^2}{\nu},\ \omega = \frac{\nu\omega^*}{w_0^2},$$

$$\theta = \frac{\kappa(T^* - T_\infty^*)w_0}{q_w^* \nu},\ k = \frac{w_0^2 k^*}{\nu^2},\ \mathrm{R(rotation\ parameter)} = \frac{\Omega\nu}{w_0^2},$$

$$\alpha\ (\mathrm{thermaldiffusivity}) = \frac{\kappa}{\rho C_p},\ \mathrm{Gr\ (Grash\ of\ number)} = \frac{g\beta q_w^* \nu^2}{w_0^4 \kappa},$$

$$\mathrm{Pr\ (Prandtal\ number)} = \frac{\nu}{\alpha},\quad \mathrm{Gc\ (modified\ Grash\ of\ number)} = \frac{g\beta^{-} m_w^* \nu^2}{w_0^4 D},\quad \mathrm{Sc\ (Schmidt\ number)} = \frac{\nu}{D},\ \mathrm{E(radiationparameter)} = \frac{4\nu I}{\rho C_p w_0^2},\ \mathrm{M(Hartmannnumber)} = \sqrt{\frac{\sigma B^2 \nu}{\rho w_0^2}}$$

and

$$\gamma(\mathrm{dimension\ less\ chemical\ reaction\ parameter}) = \frac{k_1 \nu}{w_0^2}.$$

The radiative heat flux, as ascertained in the study of Cogley et al. [59], can be expressed in the following form:

$$\frac{\partial q_r^*}{\partial z^*} = 4(T^* - T_\infty^*)I^*,$$
$$I^* = \int_0^\infty \kappa_{\lambda\omega} \frac{\partial e_{b\lambda}}{\partial T^*} d\lambda,$$

where $\kappa_{\omega\lambda}$is the absorption coefficient at the wall, $e_{b\lambda}$ is Planck's function.

Now, substituting the dimensionless quantities in Eqs (13), (9) and (10), the resultantly obtained dimensionless equations are:

$$\frac{\partial U}{\partial t} - \frac{\partial U}{\partial z} + 2i\,\mathrm{RU} = \mathrm{Gr}\,\theta + GcC + \frac{\partial^2 U}{\partial z^2} - \frac{U}{k} - M^2 U, \quad (14)$$

$$\frac{\partial \theta}{\partial t} - \frac{\partial \theta}{\partial z} = \frac{1}{Pr\frac{\partial^2 \theta}{\partial z^2}} \quad (15)$$

$$\frac{\partial C}{\partial t} - \frac{\partial C}{\partial z} = \frac{1}{Sc}\frac{\partial^2 C}{\partial z^2} - \gamma C, \quad (16)$$

and the corresponding boundary conditions of the problem embodied in Eq. (11) are mentioned by:

$$\left.\begin{array}{l} z = 0 : U = 0,\ \frac{\partial \theta}{\partial z} \\ \quad = -(1 + \varepsilon e^{i\omega t}), \frac{\partial C}{\partial z} \\ \quad = -(1 + \varepsilon e^{i\omega t}) \\ z \to \infty : U \to 0, \theta \to 0, C \to 0. \end{array}\right\} \quad (17)$$

### 2.1. Solution of the problem

Since the amplitude ε (< < 1) of the variation is extremely small, we accordingly consider the solutions of the problem in the following arrangement:

$$\left.\begin{array}{l} U(z,t) = U_0(z) + \varepsilon U_1(z) e^{i\omega t} + \ldots\ldots\ldots\ldots \\ \theta(z,t) = \theta_0(z) + \varepsilon \theta_1(z) e^{i\omega t} + \ldots\ldots\ldots\ldots \\ C(z,t) = C_0(z) + \varepsilon C_1(z) e^{i\omega t} + \ldots\ldots\ldots\ldots \end{array}\right\} \quad (18)$$

Substituting Eq. (18) in Eqs (14)–(16), and equating it to the coefficients of various powers of ε along with ignoring $\varepsilon^2, \varepsilon^3 \ldots$, we thus obtain:

$$U_0'' + U_0' - 2iR\,U_0 - \frac{U_0}{k} - M^2 U_0 = -Gr\theta_0 - GcC_0, \quad (19)$$

$$U_1'' + U_1' - 2iR\,U_1 - i\omega\,U_1 - \frac{U_1}{k} - M^2 U_1 = -Gr\theta_1 - GcC_1, \quad (20)$$

$$\theta_0'' + Pr\,\theta_0' - E\,Pr\,\theta_0 = 0, \quad (21)$$

$$\theta_1'' + Pr\theta_1' - (E + i\omega)\theta_1 Pr\ 0\ . \quad (22)$$

$$C_0'' + Sc\,C_0' - \gamma Sc C_0 = 0, \quad (23)$$

$$C_1'' + Sc\,C_1' - i\omega\,Sc C_1 - \gamma Sc C_1 = 0\ . \quad (24)$$

The analogous boundary conditions Eq. (17) come in order to the following:

$$\left.\begin{array}{l} \mathrm{z} = 0 : U_0 = 0, U_1 = 0, \frac{\partial \theta_0}{\partial z} = -1, \frac{\partial \theta_1}{\partial z} = -1, \frac{\partial C_0}{\partial z} = -1, \frac{\partial C_1}{\partial z} = -1, \\ \mathrm{z} \to \infty : U_0 \to 0, U_1 \to 0, \theta_0 \to 0, \theta_1 \to 0, C_0 \to 0, C_1 \to 0. \end{array}\right\} \quad (25)$$

Solving Eqs (19)–(24) subject to the analogous boundary conditions expressed in Eq. (25), we obtain:

$$U_0(z) = a_3(e^{-a_1 z} - e^{-a_2 z}) + a_4(e^{-b_1 z} - e^{-a_2 z}) \quad (26)$$

$$U_1(z) = \mathrm{a}_8(e^{-a_5 z} - e^{-a_7 z}) + a_9(e^{-a_6 z} - e^{-a_7 z}) \quad (27)$$

$$\theta_0(z) = \frac{1}{a_1}\,\mathrm{e}^{-a_1 \mathrm{z}}, \quad (28)$$

$$\theta_1(z) = \frac{1}{a_5} e^{-a_5 z}. \quad (29)$$

$$C_0(z) = \frac{1}{b_1}\,\mathrm{e}^{-b_1 \mathrm{z}}, \quad (30)$$

$$C_1(z) = \frac{1}{a_6}\,\mathrm{e}^{-a_6 \mathrm{z}}, \quad (31)$$

where,

$$a_1 = \frac{1}{2}\left[Pr + \sqrt{Pr^2 + 4EPr}\right],$$
$$b_1 = \frac{1}{2}\left[Sc + \sqrt{Sc^2 + 4\gamma Sc}\right]$$
$$a_2 = \frac{1}{2}\left[1 + \sqrt{1 + 4(2iR + M^2 + \frac{1}{k})}\right]$$
$$a_3 = \frac{-\mathrm{Gr}}{a_1(a_1^2 - a_1 - (2iR + M^2 + \frac{1}{k}))},$$
$$a_4 = \frac{-\mathrm{Gc}}{b_1({b_1}^2 - b_1 - (2iR + M^2 + \frac{1}{k}))},$$
$$a_5 = \frac{1}{2}\left[Pr + \sqrt{Pr^2 + 4\,Pr(E + i\omega)}\right]$$
$$a_6 = \frac{1}{2}\left[Sc + \sqrt{Sc^2 + 4i\omega Sc}\right]$$
$$a_7 = \frac{1}{2}\left[1 + \sqrt{1 + 4(2iR + i\omega) + \frac{4}{k} + 4M^2}\right]$$
$$a_8 = \frac{-\mathrm{Gr}}{a_5(a_5^2 - a_5 - (2iR + i\omega + M^2 + \frac{1}{k}))},$$
$$a_9 = \frac{-\mathrm{Gc}}{a_6(a_6^2 - a_6 - (2iR + i\omega + M^2 + \frac{1}{k}))}.$$

### 2.2. Solution

#### 2.2.1. Steady flow

By taking $U_0 = u_0 + iv_0$ in Eq. (26), and consequently allowing for the separation of real as well as imaginary portions, the average primary $\frac{u_0}{w_0}$ and mean secondary $\frac{v_0}{w_0}$ velocity fields are ascertained as the following:

$$\left.\begin{array}{l} \frac{u_0}{w_0} = e_3(e^{-a_1 z} - e^{-e_1 z}\cos e_2 z) - e_4 e^{-e_1 z}\sin e_2 z \\ + e_5(e^{-Scz} - e^{-e_1 z}\cos e_2 z) - e_6 e^{-e_1 z}\sin e_2 z \\ \frac{v_0}{w_0} = e_4(e^{-a_1 z} - e^{-e_1 z}\cos e_2 z) + e_3 e^{-e_1 z}\sin e_2 z \\ + e_6(e^{-Scz} - e^{-e_1 z}\cos e_2 z) + e_5 e^{-e_1 z}\sin e_2 z \end{array}\right\}, \quad (32)$$

#### 2.2.2. Unsteady flow

Substituting the unsteady portions,

$U_1(z,t) = M_r + iM_i, C_1(z,t) = C_r + iC_i \mathrm{and} \theta_1(z,t) = T_r + iT_i$, respectively, in Eqs (27), (29) and (31), we obtain:

$$[U(z,t),\theta(z,t),C(z,t)] = [U_0(z),\theta_0(z)] + \varepsilon e^{i\omega t}[(M_r + iM_i),(T_r + iT_i),(C_r + iC_i] \quad (33)$$

The primary velocity, secondary velocity and temperature along with concentration areas in the components terms with fluctuation are given by:

$$\frac{u}{w_0}(z,t) = u_0 + \varepsilon(M_r \cos\omega t - M_i \sin\omega t) \quad (34)$$

$$\frac{v}{w_0}(z,t) = v_0 + \varepsilon(M_r \sin\omega t + M_i \cos\omega t) \quad (35)$$

$$\theta(z,t) = \theta_0 + \varepsilon(T_r \cos\omega t - T_i \sin\omega t) \quad (36)$$

$$C(z,t) = C_0 + \varepsilon(C_r \cos\omega t - C_i \sin\omega t) \quad (37)$$

Taking $\omega t = \frac{\pi}{2}$ in Eqs (34)–(37), we obtain the transient expressions for the primary velocity, secondary velocity and temperature, as well as the concentration, as the following:

$$\frac{u}{w_0}\left(z,\frac{\pi}{2\omega}\right) = u_0(z) - \varepsilon M_1(z), \quad (38)$$

$$\frac{v}{w_0}\left(z,\frac{\pi}{2\omega}\right) = v_0(z) + \varepsilon M_r(z), \quad (39)$$

$$\theta\left(z,\frac{\pi}{2\omega}\right) = \theta_0(z) - \varepsilon T_i(z). \quad (40)$$

$$C\left(z,\frac{\pi}{2\omega}\right) = C_0(z) - \varepsilon C_i(z). \quad (41)$$

where

$$M_r = e_{17}[e^{-e_7 z}\cos e_8 z - e^{-e_{11} z}\cos e_{12} z] - e_{18}[-e^{-e_7 z}\sin e_8 z + e^{-e_{11} z}\sin e_{12} z] + e_{23}[e^{-e_9 z}\cos e_{10} z - e^{-e_{11} z}\cos e_{12} z] - e_{24}[-e^{-e_9 z}\sin e_{10} z + e^{-e_{11} z}\sin e_{12} z]$$

$$M_i = e_{17}[-e^{-e_7 z}\sin e_8 z + e^{-e_{11} z}\sin e_{12} z] + e_{18}[e^{-e_7 z}\cos e_8 z - e^{-e_{11} z}\cos e_{12} z] + e_{23}[-e^{-e_9 z}\sin e_{10} z + e^{-e_{11} z}\sin e_{12} z] + e_{24}[e^{-e_9 z}\cos e_{10} z - e^{-e_{11} z}\cos e_{12} z]$$

$$T_i = -\frac{e^{-e_7 z}}{e_7^2 + e_8^2}[-e_8\cos e_8 z - e_7 \sin e_8 z]$$

$$C_i = \frac{e^{-e_9 z}}{e_9^2 + e_{10}^2}[-e_9 \sin e_{10} z - e_{10}\cos e_{10} z]$$

$$a_2 = e_1 + ie_2, a_3 = e_3 + ie_4, a_4 = e_5 + ie_6, a_5 = e_7 + ie_8, a_6 = e_9 + ie_{10}, a_7 = e_{11} + ie_{12}, a_8 = e_{17} + ie_{18}, a_9 = e_{23} + ie_{24}$$

$$e_1 = \frac{1}{2}\left[1 + \sqrt{\sqrt{[1+4(M^2+\frac{1}{k})]^2 + 64R^2}\,\frac{[1+4(M^2+\frac{1}{k})]^2 - 64R^2}{[1+4(M^2+\frac{1}{k})]^2 + 64R^2}}\right]$$

$$e_2 = \frac{1}{2}\sqrt{\sqrt{[1+4(M^2+\frac{1}{k})]^2 + 64R^2}\,\frac{16R[1+4(M^2+\frac{1}{k})]}{[1+4(M^2+\frac{1}{k})]^2 + 64R^2}}$$

$$e_3 = -\frac{Gr[a_1^3 - a_1^2 - (M^2+\frac{1}{k})a_1]}{[a_1^3 - a_1^2 - (M^2+\frac{1}{k})a_1]^2 + 4R^2 a_1^2}$$

$$e_4 = -\frac{2Ra_1 Gr}{[a_1^3 - a_1^2 - (M^2+\frac{1}{k})a_1]^2 + 4R^2 a_1^2}$$

$$e_5 = -\frac{Gc[Sc^3 - Sc^2 - (M^2+\frac{1}{k})Sc]}{[Sc^3 - Sc^2 - (M^2+\frac{1}{k})Sc]^2 + 4R^2 Sc^2}$$

$$e_6 = -\frac{2RScGc}{[Sc^3 - Sc^2 - (M^2+\frac{1}{k})Sc]^2 + 4R^2 Sc^2}$$

$$e_7 = \frac{1}{2}Pr + \sqrt{\sqrt{(Pr^2 + 4E\,Pr)^2 + 16\omega^2 Pr^2}.\frac{(Pr^2+4E\,Pr)^2 - 16\omega^2 Pr^2}{(Pr^2+4E\,Pr)^2 + 16\omega^2 Pr^2}}$$

$$e_8 = \frac{1}{2}\sqrt{\sqrt{(Pr^2 + 4E\,Pr)^2 + 16\omega^2 Pr^2}.\frac{8\,Pr\,\omega(Pr^2+4E\,Pr)}{(Pr^2+4E\,Pr)^2 + 16\omega^2 Pr^2}}$$

$$e_9 = \frac{1}{2}\left[Sc + \sqrt{\sqrt{Sc^4 + 16\omega^2 Sc^2}.\frac{Sc^4 - 16\omega^2 Sc^2}{Sc^4 + 16\omega^2 Sc^2}}\right]$$

$$e_{10} = \frac{1}{2}\left[\sqrt{\sqrt{Sc^4 + 16\omega^2 Sc^2}.\frac{8\omega Sc^3}{Sc^4 + 16\omega^2 Sc^2}}\right]$$

$$e_{11} = \frac{1}{2}\left[1 + \sqrt{\sqrt{(1+\frac{4}{k}+4M^2)^2 + (8R+4\omega)^2}.\frac{(1+\frac{4}{k}+4M^2)^2 - (8R+4\omega)^2}{(1+\frac{4}{k}+4M^2)^2 + (8R+4\omega)^2}}\right]$$

$$e_{12} = \frac{1}{2}\left[\sqrt{\sqrt{(1+\frac{4}{k}+4M^2)^2 + (8R+4\omega)^2}.\frac{2(1+\frac{4}{k}+4M^2)(8R+4\omega)}{(1+\frac{4}{k}+4M^2)^2 + (8R+4\omega)^2}}\right]$$

$$e_{13} = e_7^2 - e_8^2 - e_7 - M^2 - \frac{1}{k}, e_{14} = 2e_7 e_8 - e_8 - 2R - \omega$$

$$e_{15} = e_7 e_{13} - e_8 e_{14}, e_{16} = e_8 e_{13} + e_7 e_{14}, e_{17} = -\frac{Gre_{15}}{e_{15}^2 + e_{16}^2}, e_{18} = \frac{Gre_{16}}{e_{15}^2 + e_{16}^2}$$

$$e_{19} = e_9^2 - e_{10}^2 - e_9 - M^2 - \frac{1}{k}, e_{20} = 2e_9 e_{10} - e_{10} - 2R - \omega$$

$$e_{21} = e_9 e_{19} - e_{10} e_{20}, e_{22} = e_{10} e_{19} - e_9 e_{20}, e_{23} = -\frac{Gce_{21}}{e_{21}^2 + e_{22}^2}, e_{24} = \frac{Gre_{22}}{e_{21}^2 + e_{22}^2}.$$

It is critical to understand the impact of the Grashoff numbers and magnetic field on mean skin-friction at $z = 0$ after learning about the mean flow velocity field, and the same is provided in the form:

$$\tau * = \mu\left(\frac{dU^*}{dz^*}\right)_{z*=0}, \quad (42)$$

Further, in non-dimensional form, it is provided as follows:

$$\tau = \frac{\tau^* v}{\mu w_0^2} = \left(\frac{\partial U}{\partial z}\right)_{z=0} = \left(\frac{\partial U_0}{\partial z}\right)_{z=0} + \varepsilon\left(\frac{\partial U_1}{\partial z}\right)_{z=0} e^{iwt}. \quad (43)$$

We denote the mean skin-friction by:

$$\tau_m = \left(\frac{du_0}{dz}\right)_{z=0}. \quad (44)$$

Now, after having ascertained the temperature field, we move on to examining how the rate of heat transfer is affected by ω. The Nusselt number can be used to calculate the rate of heat transfer.

$$Nu = -\frac{q_\omega^* v}{k\, w_0\,(T^* - T_\infty^*)} = \left(\frac{\partial\theta}{\partial z}\right)_{z=0} = \left(\frac{\partial\theta_0}{\partial z}\right)_{z=0} + \varepsilon\left(\frac{\partial\theta_1}{\partial z}\right)_{z=0} e^{i\omega t} \quad (45)$$

## 3. VALIDATION

To validate the findings of the present work vis-à-vis those of Sharma et al. [50] (while neglecting the rotation and radiation effect), a comparison of the velocity and transient temperature profiles is carried out, as indicated in Figs. 2 and 3. It is observed that there is good agreement between the present work and the previous research.

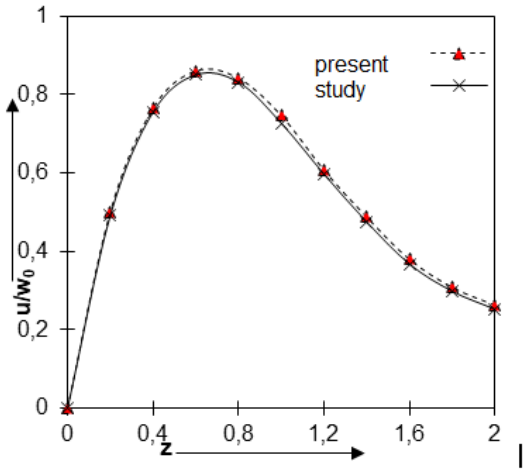


**Fig. 2.** Comparative analysis of mean primary velocity profile

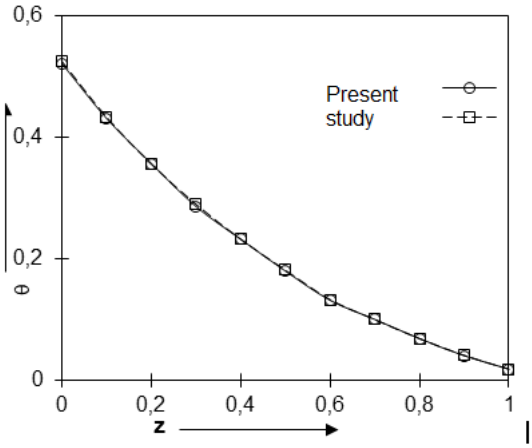


**Fig. 3.** Comparative analysis of transient temperature profiles

## 4. GRAPHICAL PRESNTATION AND DISCUSSION

After obtaining the various flow characteristics, the numerical calculations are made for the various numerical solutions of the thermal Grashoff number 'Gr', the solutal Grashoff number 'Gc', the Schmidt number 'Sc', the frequency $\omega$, the permeability parameter k, the radiation parameter E and the Hartmann number (a magnetic field parameter) M. Approximately 0.71 is taken as the Prandtl, which, in the air, is designated at 20°C. The Schmidt numbers are considered in the study to show the utmost common diffusive chemical species present in the air. The values of the Schmidt number 'Sc' are 0.60 and 1.002 in the air, which represents the species $H_2O$ and $CO_2$ in the air at 25°C and 1 atmospheric pressure. The values of various numbers such as Gc, Gr, k, M, $\omega$ and E are determined based on the own judgement of the present researchers.

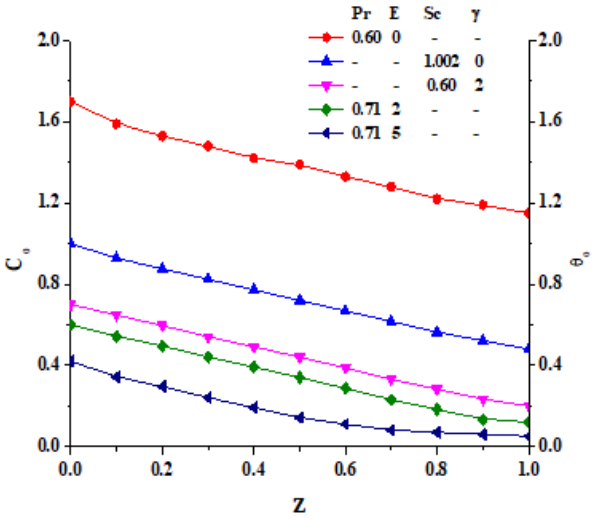


**Fig. 4.** Mean temperature and mean concentration profiles

It has been noted from Eq. (26) that the steady state portion of the average primary velocity value for its field is having a two-layer characteristic, and these two layers been acknowledged as the suction and thermal layers. The existence of the suction layer is because of the revolution and medium porousness, while the thermal layer exists because of an interplay of the thermal field generated by the radiation heat transfer and the velocity related to its field, as reported by Cogley et al. [59] and Xin et al. [60]; however, this interplay depends upon the Grashof number as well as the radiation parameters.

The profiles of the mean temperature as well as the mean concentration are represented in Fig. 4. It has been sighted that the mean temperature as well as the mean concentration decreases exponentially. The mean temperature reduces with the rise in the radiation-pertaining parameter E. From the quality point of view, the results are acceptable with some exceptions, since, due to the impact of the radiative heat transfer, the rate of energy transportation to the relevant fluid reduces with the reduction of the temperature of the fluid.

It has been perceived as well from Fig. 4 that the mean level of the concentration for the fluid decreases with the upturn in the Schmidt number, which indicates that the mass diffusivity increases the concentration level with steady rate. Moreover, it is also detected from Fig. 1 that there was a fall in the concentration under the impact of the parameter $\gamma$ related to the chemical reaction. Similar trends can be observed in the researches of Sharma and Gandhi [61] and Li et al. [62].

The mean and transient primary velocities are presented in Figs. 5 and 7 for arbitrary values of the thermal Grashof number Gr = 2, the parameter related to permeability k = 0.5, the rotation parameter R = 2 and the Prandtl number Pr = 0.71 (air). The Grashof number 'Gc' is expressed by the ratio between the buoyancy force species and the hydrodynamic force due to viscosity. It has been observed that the mean and transient primary velocities rise significantly with an increase of the buoyancy force for species, and this phenomenon is in good agreement with the findings of Sharma et al. [63]. The mean and transient primary velocities are supposed to drop along with the upsurge of the parameter M of the magnetic field. This happens due to the use of the magnetic

DOI 10.2478/ama-2024-0023



field in the transverse direction, the consequence of which is the production of a resistive kind of force known as the Lorentz force. This is similar to a drag force, and it has a tendency to oppose the flow of fluid, together with a subsequent reduction in its velocity.

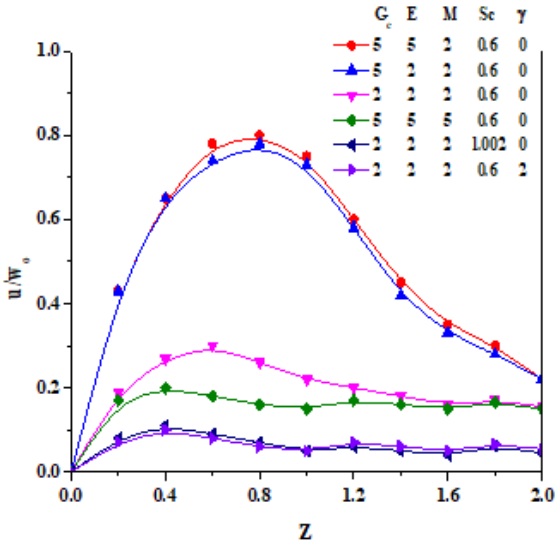


**Fig. 5.** Mean primary velocity profiles for Gr = 2, k = 0.5, R = 2 and Pr = 0.71

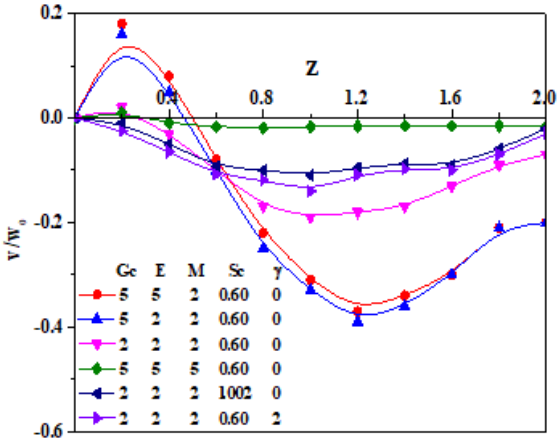


**Fig. 6.** Mean secondary velocity profiles for Gr = 2, k = 0.5, R = 2 and Pr = 0.71.

Fig. 6 demonstrates the variation of the profiles pertaining to the mean secondary velocity with the variation of the various parameters. It is seen that the mean secondary velocity rises both with increasing E and M. Interestingly, it has been found that the secondary velocity rises due to Gc close to the plate and then reduces remotely from the upright plate.

It is also observed that the mean secondary velocity falls under the effect of the Schmidt number 'Sc'. Interestingly, it is noted that the mean secondary velocity initially fall under the impact of the chemical reaction parameter $\gamma$, while a reverse impact is seen remotely from the plate. It has also been perceived that the mean and transient primary velocities become subject to upsurges with the radiation parameter E, while reverse phenomena are observed for the Schmidt number 'Sc' along with the chemical reaction parameter $\gamma$. Moreover, from Fig. 7, we infer that the transient primary velocity accelerates with frequency of oscillation $\omega$.

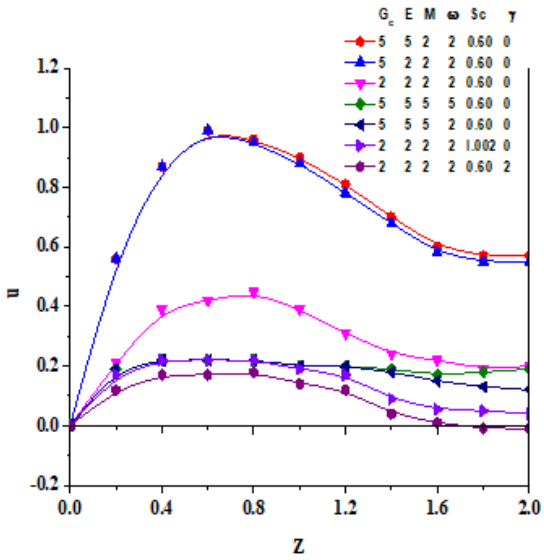


**Fig. 7.** Transient primary velocity profiles for Gr = 2, k = 0.5, ε = 2 and Pr = 0.71

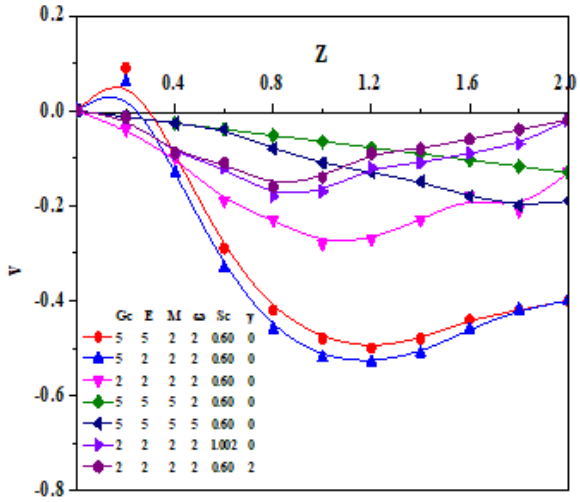


**Fig. 8.** Transient secondary velocity profiles for Gr = 2, k = 0.5, Pr = 0.71, R = 2 and ε = 2

Fig. 8 exhibits the variation of transient secondary velocity against span-wise coordinate z under the influence of Gc, E, M, $\omega$ and Sc. The transient secondary velocity accelerates with the parameter M related to the magnetic field and the Schmidt number 'Sc', whereas it falls under the effect of the radiation parameter E and the frequency of fluctuation $\omega$. From Fig. 8, we observe that the transient secondary velocity underwent a rise owing to augmentation in the solutal's Grashof number 'Gc' near the plate, whereas a reverse effect was observed far away from the plate. Moreover, from Fig. 8, it is revealed that transient secondary velocity increases as rise occurs in the chemical reaction's parameter $\gamma$. This leads us to the understanding that the reduction in the chemical species directs towards a boost in the magnitude of the concentration field, and resultantly, there is an enhancement in the buoyancy impacts owing to the concentration gradients, which accelerates the fluid flow field.

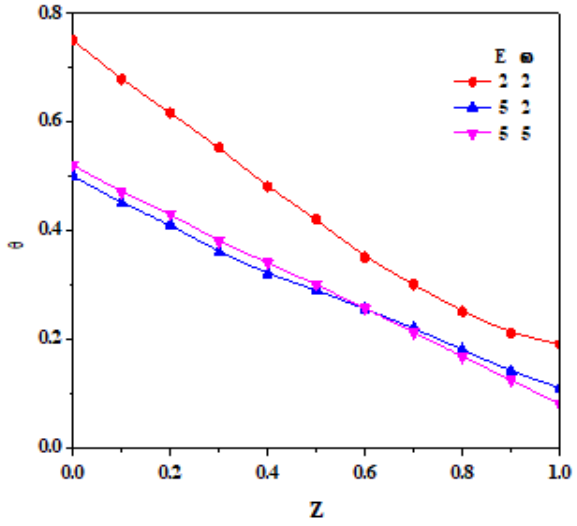


**Fig. 9.** Transient temperature profiles for Pr = 0.71 and ε = 0.2

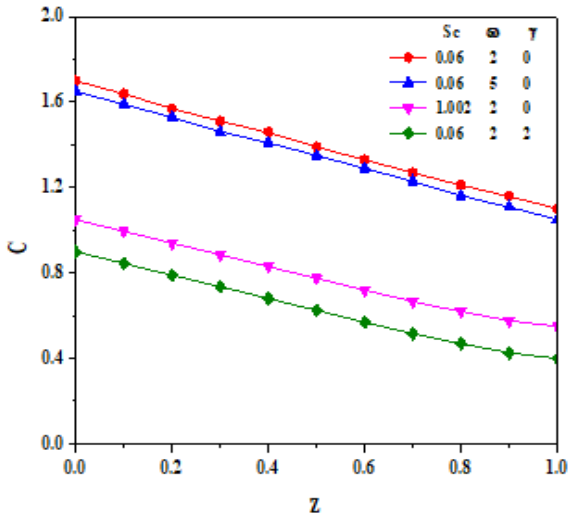


**Fig. 10.** Transient concentration profiles for ε = 0.2

A similar trend can be observed in previous studies in the literature [64–66]. The plot of the transient temperature profile for numerous values of radiation parameter as well as frequency of fluctuation is provided in Fig. 9. It is noticed that the transient temperature reduces along with the increase in the radiation parameter E, and this reduction is attributed to the fact that, under the existence of the thermal buoyancy force, the rise in the parameter E related to radiation guides towards the rise of the boundary layer concentration as well as towards the dropping of the rate of the heat flux. Further, it also ascertained that the temperature accelerated with the frequency of oscillation in the vicinage of the vertical surface, while it decelerated remotely from the plate.

Fig. 10 describes the impact of Schmidt number, frequency of fluctuation and the parameter γ related to chemical reaction on the transient concentrations. It is also ascertained from Fig. 7 that the transient concentration reduces with rising ω, γ and Sc. For the generative reaction γ > 0, while the reverse impact is detected, i.e. as soon as the reaction parameter rises, the concentration profiles become thicker, and accordingly, decreases take place in the transient concentration.

Tab. 1 illustrates the values of Nusselt number with frequency of fluctuations ω. It is observed that they behave similar to a cosine wave. Tab. 2 presents the values of mean skin-friction for different values of the magnetic field parameter M. It is observed that mean skin-friction decreases with increase in the magnetic field parameter M, for every value of the Schmidt number 'Sc'.

**Tab. 1.** Values of Nusselt number for ε = 0.2

| ω | Nu for t = 2 | Nu for t = 4 | Nu for t = 6 |
|---|---|---|---|
| 0 | –1.2 | –1.2 | –1.2 |
| 1 | 0.9167 | 0.8692 | 1.192 |
| 2 | 0.8692 | 0.9709 | 1.1687 |
| 3 | 1.192 | 1.1687 | 1.132 |
| 4 | 0.9709 | 0.8084 | 1.0848 |
| 5 | 0.8321 | 1.0816 | 1.0308 |
| 6 | 1.1687 | 1.0848 | 0.9744 |
| 7 | 1.0273 | 0.8074 | 0.92 |
| 8 | 0.8084 | 1.1668 | 0.8719 |
| 9 | 1.132 | 0.9744 | 0.8341 |
| 10 | 1.0816 | 0.8666 | 0.8095 |

**Tab. 2.** Values of $\tau_m$ (mean skin-friction) for Gr = 2, Gc = 2, E = 2, k = 0.5, Pr = 0.71 and γ = 2

| M | Sc = 0.60 | Sc = 0.78 | Sc = 1.002 |
|---|---|---|---|
| 0 | 1.053428 | 0.917919 | 0.814144 |
| 2 | 0.753157 | 0.666109 | 0.597228 |
| 4 | 0.50047 | 0.448243 | 0.405931 |
| 6 | 0.367434 | 0.331293 | 0.301715 |
| 8 | 0.288942 | 0.261552 | 0.239024 |
| 10 | 0.237704 | 0.215728 | 0.197601 |
| 12 | 0.201763 | 0.183441 | 0.168304 |
| 14 | 0.175202 | 0.159506 | 0.146524 |
| 16 | 0.154792 | 0.14107 | 0.129711 |
| 18 | 0.138624 | 0.126439 | 0.116347 |
| 20 | 0.125506 | 0.114549 | 0.105471 |

## 5. CONCLUSIONS

Assuming the periodical thermal and mass diffusion at the upright surface, the investigational solutions are found for flow characteristics by following the regular perturbation method, and the impact of different parameters on flow-related characteristics are explained and depicted graphically. The results may be useful in studying oil or gas and water movement through an oil or gas field reservoir, underground water migration, and the filtration and water purification processes.

- The mean and transient primary velocities step-up significantly with the increase of the species buoyancy force, while a reverse response is observed for the magnetic field parameter M.
- It has also been noticed that the mean and transient primary velocities rise with the radiation parameter E, while reverse phenomena are observed for the Schmidt number 'Sc' and the parameter γ pertaining to chemical reaction.
- The temperature profile accelerated with frequency of oscillation near the plate, whereas it decelerated far away from plate.

- It has been observed that transient temperature falls with rise in the parameter related to radiation.
- The transient concentration drops with increasing $\omega$, $\gamma$ and Sc.

## REFERENCES

1. Gebhart B, Pera L. The nature of vertical natural convection flow from the combined buoyancy effects-on thermal and mass diffusion. Int. J. Heat Mass Transfer. 1971; 14: 2024-2050 http://dx.doi.org/10.1016/0017-9310(71)90026-3.
2. Khanduri U, Sharma BK, Sharma M, Mishra NK, Saleem N. Sensitivity analysis of electroosmotic magnetohydrodynamics fluid flow through the curved stenosis artery with thrombosis by response surface optimization. Alexandria Engineering Journal, 2023: 75, 1-27. https://doi.org/10.1016/j.aej.2023.05.054.
3. Kodi R, Ganteda C, Dasore A, Kumar ML, Laxmaiah G, Hasan MA, Islam S, Razak A. Influence of MHD mixed convection flow for maxwell nanofluid through a vertical cone with porous material in the existence of variable heat conductivity and diffusion. Case Studies in Ther Engg. 2023; 44: 102875.
4. Veera Krishna M, Chamkha AJ. Hall and ion slip effects on magnetohydrodynamic convective rotating flow of Jeffreys fluid over an impulsively moving vertical plate embedded in a saturated porous medium with Ramped wall temperature. Numerical Methods for Partial Differential Equations. 2021; 37(3): 2150-2177. https://doi.org/10.1002/num varying concentratio.22670
5. Veera Krishna M. Hall and ion slip impacts on unsteady MHD free convective rotating flow of Jeffreys fluid with ramped wall temperature. Int. Commun in Heat and Mass Transf. 2020; 119: 107927. https://doi.org/10.1016/j.icheatmasstransfer.2020.104927
6. Hossain MA, Hussain S, Rees DAS. Influence of fluctuating surface temperature and concentration on natural convection flow from a vertical flat plate. J. of Appl. Math. and Mech. 2001; 81: 699-709. https://doi.org/10.1002/1521-4001(200110)81:10%3C699::AID-ZAMM699%3E3.0.CO;2-3
7. Sahoo SN, Rout PK, Dash GC. Unsteady MHD Flow through Porous Media with Temporal Variation in Temperature and Concentration at the Plate. Int. J. of Ambient Energy. 2022; 43(1): 7977-7986. https://doi.org/10.1080/01430750.2022.2086914
8. Sharma PK. Simultaneous thermal and mass diffusion on three-dimensional mixed convection flow through a porous medium. J. of Porous Media. 2005; 8(4): 419-427. doi:10.1615/JPorMedia.v8.i4.70.
9. Maatoug S, Babu HK, Deepthi VVL. Ghachem K, Raghunath K, Ganteda CK, Khan SU. Variable chemical species and thermo-diffusion Darcy-Forchheimer squeezed flow of Jeffrey nanofluid in horizontal channel with viscous dissipation effects. J. of the Indian Chem. Society. 2023; 100(1): 100831.
10. Deepthi VVL, Lashin MMA, Kumar NR, Raghunath K, Ali F, Oreijah M, Guedri K, Tag-ElDin ESM, Khan MI, Galal AM. Recent Development of Heat and Mass Transport in the Presence of Hall, Ion Slip and Thermo Diffusion in Radiative Second Grade Material: Application of Micromachines. *Micromachines.* 2022; *13*(10): 1566. https://doi.org/10.3390/mi13101566
11. Chu YM, Jakeer S, Reddy SRR, Rupa ML, Trabelsi Y, Khan MI, Hejazi HA, Makhdoum BM. Eldin S.M. Double diffusion effect on the bio-convective magnetized flow of tangent hyperbolic liquid by a stretched nano-material with Arrhenius Catalysts. Case Studies in Thermal Engg. 2023; 44: 102838. https://doi.org/10.1016/j.csite.2023.102838
12. Sharma BK, Sharma PK, Chaudhary RC. Effects of fluctuating surface temperature and concentration on unsteady convection flow past an infinite vertical plate with constant suction. Heat Transf. Res. 2009; 40(6): 505-519. doi: 10.1615/HeatTransRes.v40.i6.10.
13. Shuguang Li, Kodi R, Ayman A, Farhan A, Zaib A, Khan MI, Sayed M E & Puneeth V. Effects of activation energy and chemical reaction on unsteady MHD dissipative Darcy-Forchheimer squeezed flow of Casson fluid over horizontal channel. Sc. Report. 2023:13: 2666.
14. Bafakeeh OT, Raghunath K, Ali F, Khalid M, Tag-ElDin ESM, Oreijah M, Guedri K, Kheder NB, Khan MI. Hall Current and Soret Effects on Unsteady MHD Rotating Flow of Second-Grade Fluid through Porous Media under the Influences of Thermal Radiation and Chemical Reactions. *Catalysts.* 2022; *12*(10): 1233. https://doi.org/10.3390/catal12101233
15. Raghunath K, Mohanaramana R. Hall, Soret, and rotational effects on unsteady MHD rotating flow of a second-grade fluid through a porous medium in the presence of chemical reaction and aligned magnetic field. Int. Commun in Heat and Mass Transf. 2022; 137: 106287. https://doi.org/10.1016/j.icheatmasstransfer.2022.106287
16. Tripathi B, Sharma BK. Effect of variable viscosity on MHD inclined arterial blood flow with chemical reaction. Int. J. of Appl. Mech. and Engg. 2018; 23(3): 767–785. http://dx.doi.org/10.2478/ijame-2018-0042.
17. Tripathi B, Sharma BK. Influence of heat and mass transfer on two-phase blood flow with joule heating and variable viscosity in the presence of variable magnetic field. Int. J. of Comput. Method. 2020; 17(3): 1850139. https://doi.org/10.1142/S0219876218501396
18. Li S, Khan MI, Alzahrani F, Eldin SM. Heat and mass transport analysis in radiative time dependent flow in the presence of Ohmic heating and chemical reaction, viscous dissipation: An entropy modelling. Case Studies in Thermal Engg. 2023; 42: 102722. https://doi.org/10.1016/j.csite.2023.102722
19. Li S, Raghunath K, Alfaleh A, Ali F, Zaib A, Khan MI, Eldin SM, Puneeth V. Effects of activation energy and chemical reaction on unsteady MHD dissipative Darcy–Forchheimer squeezed flow of Casson fluid over horizontal channel. Scientific reports. 2023; 13: 2666. https://doi.org/10.1038/s41598-023-29702-w
20. Chamka AJ, Takhar HS, Soundalgekar VM. Radiation effects on free convection flow past a semi-infinite vertical plate with mass transfer. Chem. Engg. J. 2001; 84: 335-342. http://dx.doi.org/10.1016/S1385-8947(00)00378-8
21. Chamka AJ. Non-Darcy fully developed mixed convection in a porous medium channel with heat generation/absorption and hydromagnetic effects. Numer. Heat transfer. 1997; 32: 853-875. https://doi.org/10.1080/10407789708913911
22. Chamka AJ, Mujtaba M, Quadri A, Issac C. Thermal radiation effects on MHD forced convection flow adjacent to a non-isothermal wedge in the presence of heat source or sink. Heat Mass Transfer. 2003; 39: 305-312. https://doi.org/10.1007/s00231-002-0353-4.
23. Kumar YS, Hussain S, Raghunath K, Farhan A, Kamel G, Sayed M, Khan MI. Numerical analysis of magnetohydrodynamics Casson nanofluid flow with activation energy, Hall current and thermal radiation. Sc. Report. 2023:13: 4021.
24. Kodi R. Study of Heat and Mass Transfer of an Unsteady Magneto-hydrodynamic Nanofluid Flow Past a Vertical Porous Plate in the Presence of Chemical Reaction, Radiation and Soret Effects. J. of Nanofluids. 2023; 12(3): 767-776(10). https://doi.org/10.1166/jon.2023.1965
25. Veera Krishna M, Jyothi K, Chamkha AJ. Heat and mass transfer on MHD flow of second-grade fluid through porous medium over a semi-infinite vertical stretching sheet. J. of Porous Media. 2020; 23(8): 751-765.10.1615/JPorMedia.2020023817.
26. Muthucumaraswamy R, Senthil Kumar G. Heat and mass transfer effects on moving vertical plate in the presence of thermal radiation. Theor. Appl. Mech. 2004; 31: 35-46. http://dx.doi.org/10.2298/TAM0401035M
27. Muthucumaraswamy R, Chandrakala P. Radiative heat and mass transfer effects on moving isothermal vertical plate in the presence of chemical reaction. Int. J. of Appl. Mech. and Engg. 2006; 11: 639-646.
28. http://www.ijame.uz.zgora.pl/ijame_files/archives/v11PDF/n3/639-646_Article_16.pdf.

29. Veera Krishna M, Jyothi K, Chamkha AJ. Heat and mass transfer on unsteady, magnetohydrodynamic, oscillatory flow of second-grade fluid through a porous medium between two vertical plates, under the influence of fluctuating heat source/sink, and chemical reaction. Int. J. of Fluid Mechanics Research. 2018; 45(5): 459-477. 10.1615/InterJFluidMechRes.2018024591.
30. Veera Krishna M, Anand PVS, Chamkha AJ. Heat and mass transfer on free convective flow of a micropolar fluid through a porous surface with inclined magnetic field and hall effects. Special topics & Reviews in the porous media: An Int. J. 2019; 10(3): 203-233. 10.1615/SpecialTopicsRevPorousMedia.2018026943.
31. Prasad VR, Reddy NB. Radiation and mass transfer effects on an unsteady MHD free convection flow past a heated vertical plate in a porous medium with viscous dissipation. Theoret. Appl. Mech. 2007; 34(2): 135-160. https://doi.org/10.2298/TAM0702135P.
32. Prasad VR, Reddy NB, Muthucumaraswamy R. Radiation and mass transfer effects on two-dimensional flow past an impulsively started infinite vertical plate. Int. J. of Therm. Science. 2007; 46(12): 1251-1258. http://dx.doi.org/10.1016/j.ijthermalsci.2007.01.004.
33. Baitharu AP, Sahoo SN, Dash GC. Numerical approach to non-Darcy mixed convective flow of non-Newtonian fluid on a vertical surface with varying surface temperature and heat source. Karabala Int. J. of Modern Sc. 2020; 6(3): 332-343. https://doi.org/10.33640/2405-609X.1753.
34. Krishna MV, Ahamad NA, Chamkha AJ. Numerical investigation on unsteady MHD convective rotating flow past an infinite vertical moving porous surface. Ain Shams Engg. J. 2021; 12(2): 2099-2109. https://doi.org/10.1016/j.asej.2020.10.013
35. Li S, Ali F, Zaib A, Loganathan K, Eldin SM, Khan MI. Bioconvection effect in the Carreau nanofluid with Cattaneo–Christov heat flux using stagnation point flow in the entropy generation: Micromachines level study. Open Physics. 2023; 21(1): 20220228. https://doi.org/10.1515/phys-2022-0228
36. Hossain MA, Das SK, Pop I. Heat transfer response of MHD free convection flow along a vertical plate to surface temperature oscillation. Int. J. Non-linear Mech. 1998; 33: 541-553. https://doi.org/10.1016/S0020-7462(96)00151-5
37. Reddy Vaddemani R, Kodi R, Mopuri O. Characteristics of MHD Casson fluid past an inclined vertical porous plate. Materialstoday: Proceedings. 2022; 49(5): 2136-2142. https://doi.org/10.1016/j.matpr.2021.08.328
38. Veera Krishna M, Chamkha AJ. Hall and ion slip effects on MHD rotating boundary layer flow of nanofluid past an infinite vertical plate embedded in a porous medium. Results in Physics. 2019; 15: 102652. https://doi.org/10.1016/j.rinp.2019.102652
39. Veera Krishna M. Hall and ion slip effects on radiative MHD rotating flow of Jeffreys fluid past an infinite vertical flat porous surface with ramped wall velocity and temperature. Int. Commun in Heat and Mass Transf. 2021; 126: 105399. https://doi.org/10.1016/j.icheatmasstransfer.2021.105399
40. Veera Krishna M, Chamkha AJ. Hall and ion slip effects on MHD rotating flow of elastico-viscous fluid through porous medium. Int. Commun in Heat and Mass Transf. 2020; 113: 104494. https://doi.org/10.1016/j.icheatmasstransfer.2020.104494
41. Sharma BK, Mishra A, Gupta S. Heat, and mass transfer in magneto-biofluid flow through a non-Darcian porous medium with joule effect. J. of Engg. Physics and Thermophys. 2013; 86(4): 766–774. http://dx.doi.org/10.1007/s10891-013-0893-0
42. Rout PK, Sahoo SN, Dash GC. Effect of Heat Source and Chemical Reaction on MHD Flow Past a Vertical Plate with Variable Temperature. J. of Naval Architec. and Marine Engg. 2016; 13(1): 101-110. https://doi.org/10.3329/jname.v13i1.23930
43. Aldoss TK, Al-Nimr A, Jarrah MA, Al-Sha'er BJ. Magnetohydrodynamic mixed convection from a vertical plate embedded in a porous medium. Numerical Heat Transfer Part A. 1995; 28(5): 635–645. https://doi.org/10.1080/10407789508913766.
44. Helmy KA. MHD unsteady free convection flow past a vertical porous plate. ZAMM. 1998; 78(4): 255–270. https://doi.org/10.1002/(SICI)1521-4001(199804)78:4%3C255::AID-ZAMM255%3E3.0.CO;2-V
45. Kim YJ. Unsteady MHD convective heat transfer past a semi-infinite vertical porous moving plate with variable suction. Int. J. of Engg. Sc. 2000; 38(8): 833–845. http://dx.doi.org/10.1016/S0020-7225(99)00063-4
46. Veera Krishna M, Swarnalathamma BV, Chamkha AJ. Investigations of Soret, Joule and Hall effects on MHD rotating mixed convective flow past an infinite vertical porous plate. J. of Ocean Engg. and Sc. 2019; 4(3): 263-275. https://doi.org/10.1016/j.joes.2019.05.002
47. Veera Krishna M, Ahamad NA, Chamkha AJ. Hall and ion slip effects on unsteady MHD free convective rotating flow through a saturated porous medium over an exponential accelerated plate. Alex. Engg. J. 2020; 59(2): 565-577. https://doi.org/10.1016/j.aej.2020.01.043
48. Takhar HS, Roy S, Nath G. Unsteady free convection flow over an infinite vertical porous plate due to the combined effects of thermal and mass diffusion, magnetic field and Hall currents. Heat and Mass Transfer. 2003; 39(10): 825–834. http://dx.doi.org/10.1007/s00231-003-0427-y
49. Raghunath K, Mohanaramana R, Nagesh G, Charankumar G, Khan SU, Khan MI. Hall and ion slip radiative flow of chemically reactive second grade through porous saturated space via perturbation approach. Waves in Random and Complex Media. 2022. https://doi.org/10.1080/17455030.2022.2108555.
50. 49. Kar M, Sahoo SN, Dash GC. Effect of the Hall Current and Chemical Reaction on MHD Flow along an Accelerated Porous Flat Plate with Internal Heat Absorption/ Generation. J. of Enggg Physics and Thermophysics. 2014; 87(3): 624-634. https://doi.org/10.1007/s10891-014-1099-9
51. Sharma BK , Sharma PK and Chauhan SK. Effect of MHD on unsteady oscillatory Couette flow through porous media, Int. J. of Appl. Mech. and Engg., Poland, 2022, Vol (17),1, pp 188-202.
52. Choksi VG, Singh TR. A mathematical model of imbibition phenomenon in homogeneous porous media. Special topics & Reviews in the porous media: An Int. J. 2019; 10(1): 1-13. 10.1615/SpecialTopicsRevPorousMedia.2018021445
53. Jha BK, Isah BY, Uwanta IJ. Unsteady MDH free convective Couette flow between vertical porous plates with thermal radiation. J. of king Saud University-Science. 2015; 27(4): 338-348. https://doi.org/10.1016/j.jksus.2015.06.005
54. Kiranakumar HV, Thejas R, Naveen CS, Khan MI, Prasanna GD, Reddy S, Oreijah M, Guedri K, Bafakeeh OT, Jameel M. A review on electrical and gas-sensing properties of reduced graphene oxide-metal oxide nanocomposites. Biomass Conversion and Biorefinery. 2022. https://doi.org/10.1007/s13399-022-03258-7
55. Sharma BK, Singh AP, Yadav K, Chaudhary RC. Effects of chemical reaction on magneto-micropolar fluid flow from a radiative surface with variable permeability. Int.J. of Appl. Mech. and Engg. 2013; 18(3): 833–851. http://dx.doi.org/10.2478/ijame-2013-0050.
56. Sharma BK, Sharma P, Mishra N K, Fernandez-Gamiz U. Darcy-Forchheimer hybrid nanofluid flow over the rotating Riga disk in the presence of chemical reaction: Artificial neural network approach. Alexandria Engineering Journal, 2023: 76, 101-130. https://doi.org/10.1016/j.aej.2023.06.014.
57. Baitharu AP, Sahoo SN, Dash GC. Effect of Joule Heating on Steady MHD Convective Micropolar Fluid Flow over a Stretching/Shrinking Sheet with Slip. J. of Naval Architec. and Marine Engg. 2021; 18(2): 175-186. http://dx.doi.org/10.3329/jname.v18i2
58. Suresh P, Hari Krishan Y, Sreedhar Rao R, Janardhana Reddy PV. Effect of Chemical Reaction and Radiation on MHD Flow along a moving Vertical Porous Plate with Heat Source and Suction. Int. J. of Appl. Engg. Res. 2019; 14(4): 869-876. https://www.ripublication.com/ijaer19/ijaerv14n4_04.pdf

DOI 10.2478/ama-2024-0023




59. Mamatha SU, Renuka Devi RLV, Ahammad NA, Shah NA, Rao BM, Raju CSK, Khan MI, Guedri K. Multi-linear regression of triple diffusive convectively heated boundary layer flow with suction and injection: Lie group transformations. Int. J. of Modern Physics B. 2023; 37(1): 2350007. https://doi.org/10.1142/S0217979223500078
60. Cogley AC, Vinceti WG, Gilles SE. Differential approximation for radiation transfer in a nongray near equilibrium, AIAA Journal. 1968; 6: 551-553. https://doi.org/10.2514/3.4538
61. Xin X, Khan MI, Li S. Scheduling equal-length jobs with arbitrary sizes on uniform parallel batch machines. Open Mathematics. 2023; 21: 20220562. https://doi.org/10.1515/math-2022-0562
62. Sharma BK, Gandhi R. Combined effects of Joule heating and non-uniform heat source/sink on unsteady MHD mixed convective flow over a vertical stretching surface embedded stretching in a Darcy-Forchheimer porous medium. Propulsion and Power Research. 2022; 11(2): 276-292. https://doi.org/10.1016/j.jppr.2022.06.001
63. Li S, Puneeth V, Saeed AM, Singhal A, Al-Yarimi FAM, Eldin SM. Analysis of the Thomson and Troian velocity slip for the flow of ternary nanofluid past a stretching sheet. Scientific reports. 2023; 13: 2340. https://doi.org/10.1038/s41598-023-29485-0
64. Sharma PK, Sharma BK, Mishra NK, Rajesh H. Impact of Arrhenius activation energy on MHD nano-fluid flow past a stretching sheet with exponential heat source: A modified Buongiorno's model approach. Int. J. of Modern Physics B. 2023. https://doi.org/10.1142/S0217979223502843
65. Gandhi R, Sharma BK, Mishra NK, Al-Mdallal QM. Computer simulations of EMHD Casson nanofluid Flow of blood through an irregular stenotic permeable artery. App. of Koo-Kleinstreuer-Li Corr. Nanomaterials. 2023; 13: 652. https://doi.org/10.3390/ nano13040652
66. Jahanshahi H, Yao Q, Khan MI, Moroz I. Unified neural output-constrained control for space manipulator using tan-type barrier Lyapunov function. Adv. In Space Research. 2023; 71(9): 3712-3722. https://doi.org/10.1016/j.asr.2022.11.015
67. Liu Z, Li S, Sadaf T, Khan SU, Alzahrani F, Khan MI, Eldin SM. Numerical bio-convective assessment for rate type nanofluid influenced by Nield thermal constraints and distinct slip features. Case Studies in Thermal Engg. 2023; 44: 102821. https://doi.org/10.1016/j.csite.2023.102821



Pawan Kumar Sharma: https://orcid.org/0000-0001-5055-1159

Bhupendra Kumar Sharma: https://orcid.org/0000-0002-2051-9681

Anil Kumar: https://orcid.org/0000-0003-1681-0297